Visual and Tactile-Based Terrain Analysis Using a Cylindrical Mobile Robot

Giulio Reina[1]
e-mail: giulio.reina@unile.it
University of Lecce,
Department of Innovation Engineering,
via per Arnesano, Lecce 73100, Italy

Mario M. Foglia

Annalisa Milella

Angelo Gentile

Politecnico of Bari,
Department of Mechanical and Management Engineering,
Viale Japigia 182, Bari 70126, Italy

Ground autonomous mobile robots have important applications, such as reconnaissance, patrol, planetary exploration, and military applications. In order to accomplish tasks on rough terrain, control and planning methods must consider the physical characteristics of the vehicle and of its environment. Failure to understand these characteristics could lead to vehicle endangement and consequent mission failure. This paper describes recent and current work at the Politecnico of Bari in collaboration with the University of Lecce in the area of deformable terrain mobility and sensing. A cylindrical mobile robot is presented and its rolling motion on terrain is studied from a theoretical and experimental prospect. A comprehensive model is developed taking into account the interaction of the vehicle with the terrain and the related dynamic ill effects, such as rolling resistance and slip, and it is experimentally validated. An unconventional application of the vehicle serving as a tactile sensor is discussed and experimental results are presented showing the effectiveness of the cylindrical mobile robot in estimating the properties of homogeneous, deformable terrain, which in turn can be used to assess the vehicle traversability. [DOI: 10.1115/1.2168478]

Keywords: cylindrical mobile robot, dynamic modeling, terrain sensing

1 Introduction

Mobile robots are increasingly being used in high risk rough terrain situations. There are many kinds of mobile robots that have legs, wheels, crawlers, or their combination for locomotion. However, more efficient and versatile locomotion mechanisms, providing for high mobility on rough terrain, have to be researched yet.

This paper presents a mobile robot with a cylindrical architecture employing an out-of-balance internal device as means of locomotion. We call it the Cylindrical Mobile Robot (CMR).

A few authors have proposed vehicles with spherical and cylindrical shape [1–5]. To date all the research has focused on methods for control and path planning on flat and rigid surface. These methods are not well suited to rough terrain, since they generally do not consider vehicle and terrain physical properties. Here, the dynamic ill effects occurring at the wheel-terrain interface such as rolling resistance and slip are taken into account providing a more effective model of the vehicle's behavior on deformable, soft terrain. Experimental results are presented to validate the model obtained from a prototype operating in a multi-terrain testbed. Note that this problem is of more general interest as the proposed model can be easily extended to the interaction between terrain and conventional wheels of a wheeled mobile robot.

In order to accomplish tasks in highly challenging terrains, the knowledge of local terrain properties is also critical. For example, a vehicle traversing loose sand could become entrapped more easily than a vehicle moving on a packed soil. Estimation of key soil parameters would allow the prediction of traversability of a given terrain [6]. Previous research at MIT has attempted to address this issue by developing algorithms to identify soil cohesion and internal friction angle, and explicitly estimate terrain traversability for conventional mobile robots [7]. Vibration-based terrain classification was also suggested in [8].

Here, an unconventional application of the cylindrical mobile robot as "single wheel tester" for terrain characterization and identification is investigated considering a local dynamic model of the vehicle-terrain interaction based on the classical theory of Terramechanics [6]. An experimental framework for terrain estimation is developed by observing the kinematic and dynamic behavior of the CMR through multi-sensor measurements. The paper is organized as follows. Section 2 introduces the CMR and describes the analytical study of its rolling motion on deformable soil. In Sec. 3, a feasibility study for the application of the vehicle as a tactile sensor is discussed. Finally, Sec. 4 describes detailed experimental results, which are obtained by a cylindrical prototype.

2 The Cylindrical Mobile Robot

The paper presents a cylindrical shaped vehicle which is shown in Fig. 1(*a*). The rationale behind this unconventional design is to have an external cylindrical shell that encloses a wheeled device (WD) to actuate and control the motion; the internal WD can move inside the cylindrical shell using a motorized and controlled wheel and a free wheel of guidance. A spring system keeps the drive and guidance wheels pressed on the internal track of the shell ensuring pure rolling motion without slipping. The WD is built in such a way that the center of gravity of the robot is located below the geometric center of the shell; this solution allows the vehicle to move thanks to the unbalancing of the WD with respect to the vertical posture. For example, in the configuration shown in Fig. 1(*a*), an equivalent drive torque T is produced by the shift d of the WD weight force with respect to the center of the vehicle and brings the robot to roll overcoming the rolling resistance C_t due to terrain deformability.

Such a design is very advantageous as the robot can easily restore the stable posture. Furthermore, the robot has an inherently safe form and it has an amazing capability to recover from collisions with obstacles or other robots. The entire system is enclosed within the shell providing mechanical and environmental protection.

Note that the CMR is the unidirectional implementation of a more general mobile robot presented by the authors in previous work and named the Spherical Mobile Robot [9]. The latter vehicle, shown in Fig. 1(*b*), would allow to roll in all directions using a steerable internal WD. However, this paper focuses on the potential application of the robot as tactile sensor and to this purpose the cylindrical architecture lends itself very well.

2.1 Dynamic Model. A dynamic model that takes into account vehicle-terrain interaction is critical to implement an effec-

[1]Corresponding author.

Contributed by the Dynamic Systems Division of ASME for publication in the JOURNAL OF DYNAMIC SYSTEMS, MEASUREMENT, AND CONTROL. Manuscript received March 14, 2005; final manuscript received November 19, 2005. Review conducted by Sunil k. Agrawal. Paper presented at the 2004 ASME International Mechanical Engineering Congress (IMECE2004), November 13, 2004–November 19, 2004, Anaheim, California, USA.

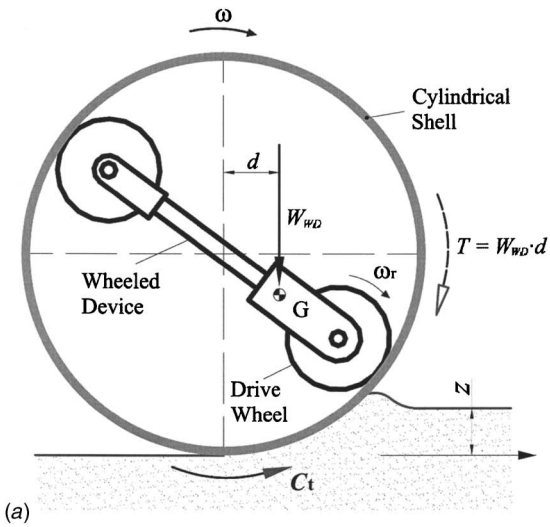

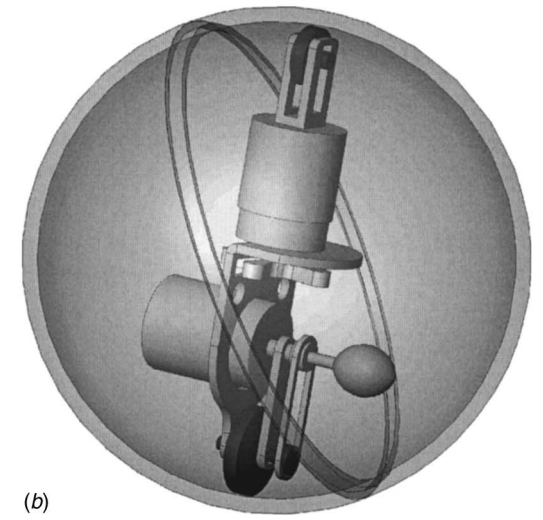

Fig. 1 The cylindrical mobile robot: (*a*) functional scheme, (*b*) mechanical design of the spherical implementation

tive control system of the vehicle on rough terrain. Conventional planning algorithms are not well suited to rough terrain, since they generally do not consider the physical capabilities of the vehicle and its environment. Failure to understand these capabilities could lead to the endangerment of the vehicle. Here, a dynamic model of the motion of the CMR on deformable, soft terrain is obtained following a Lagrange approach. The chosen Lagrange parameters are the angle β between the radius through a fixed point on the cylinder and the vertical direction, and the angle α between the same radius and the axis of the WD, as shown in Fig. 2. The difference between α and β is the swing angle of the WD within the cylindrical shell, indicated with ϕ. The following assumptions are made:

- pure rolling motion between the WD wheels and the internal track of the shell;
- the vehicle internal friction can be modeled using a viscous-Coulombian model and expressed in terms of an additional resistant torque C_o, so-defined *organic rolling resistance*; and
- any aerodynamic resistance is neglected, due to low speed range of the vehicle.

Vehicle-terrain interaction is first modeled following a global approach. In the next section, a local analysis will be also developed.

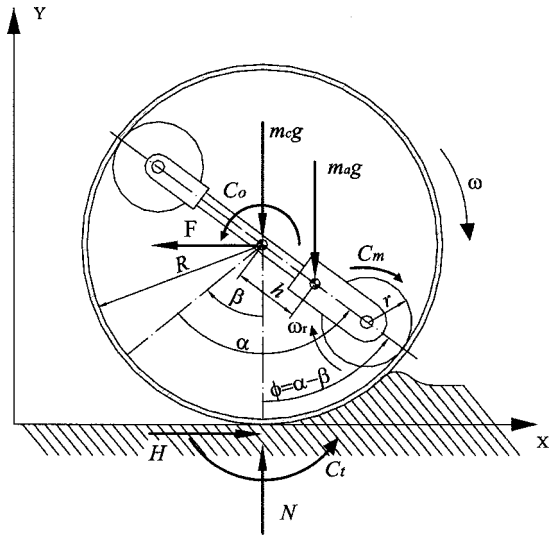

Fig. 2 Free-body diagram of the CMR

A global reaction force system composed of two forces, N and H, is assumed and a resistance torque C_t. N and H are, respectively, radial and tangential to the external shell and they can be thought of as applied at the shell bottom-dead point (see Fig. 2). C_t takes into account all energy losses at contact interface and is responsible for rolling resistance due to terrain interaction. C_t is defined as

$$C_t = f_t \cdot R \cdot W \tag{1}$$

where R is the vehicle external radius, W is the vehicle weight and f_t is an experimentally determined rolling resistance coefficient. Experimental tests indicate that f_t can be modeled using a speed-squared relationship (see Sec. 4):

$$f_t = f_o + f_s \omega^2 \tag{2}$$

where ω is the vehicle angular speed and f_o and f_s are two coefficients depending on the given terrain and so-called *basic* and *speed effect coefficient*, respectively. The kinetic energy of the cylindrical shell E_c, that of the WD E_a, that of the drive wheel E_r, and the gravity potential energy of the WD U_m, are evaluated, respectively, as

$$E_c = \frac{1}{2}(m_c R^2 + I_c) \cdot \dot{\beta}^2 \tag{3}$$

$$E_a = \frac{1}{2} I_a (\dot{\alpha} - \dot{\beta})^2 + \frac{1}{2} m_a [R^2 \dot{\beta}^2 + (\dot{\alpha} - \dot{\beta})^2 \cdot h^2 + 2(\dot{\alpha} - \dot{\beta}) \cdot R \cdot \dot{\beta} \cdot h \cdot \cos(\alpha - \beta)] \tag{4}$$

$$E_r = \frac{1}{2} I_r \omega_r^2 + \frac{1}{2} m_r R^2 \dot{\beta}^2 + \frac{1}{2} m_r (\dot{\alpha} - \dot{\beta})^2 (R - r)^2 + \dot{\beta} \cdot (\dot{\alpha} - \dot{\beta}) \cdot m_r R \cdot (R - r) \cdot \cos(\alpha - \beta) \tag{5}$$

$$U_m = g \cdot [1 - \cos(\alpha - \beta)] \cdot (m_r \cdot (R - r) + m_a \cdot h) \tag{6}$$

The meaning of the symbols used in Eqs. (3)–(6) is indicated in Fig. 2 [9]. By applying the Lagrange equation of motion

$$\frac{\partial}{\partial t}\left(\frac{\partial (E_c + E_a + E_r)}{\partial \dot{q}_i}\right) - \frac{\partial (E_c + E_a + E_r - U_m)}{\partial q_i} = t_i \quad i = 1,2 \tag{7}$$

where $q_1 = \beta$, $q_2 = \alpha$, and t_i are the nonconservative generalized forces corresponding to the chosen coordinates; after some calculations it gets

$$M(q)\ddot{q} + C(q,\dot{q})\dot{q} + h(q) = \Gamma \tag{8}$$

where

$$M(q) = \begin{bmatrix} M_{1,1} & M_{1,2} \\ M_{2,1} & M_{2,2} \end{bmatrix}, \quad C(q,\dot{q}) = \begin{bmatrix} C_{1,1} & C_{1,2} \\ C_{2,1} & C_{2,2} \end{bmatrix},$$

$$h(q) = \begin{bmatrix} h_1 \\ h_2 \end{bmatrix}, \quad \Gamma = \begin{bmatrix} t_1 \\ t_2 \end{bmatrix}$$

$$M_{1,1} = R^2(m_c + m_a + m_r) + (I_c + I_a + I_r + m_a h^2 + m_r \cdot (R-r)^2) - 2R \cdot \cos(\alpha - \beta) \cdot [(R-r) \cdot m_r + h \cdot m_a]$$

$$M_{1,2} = M_{2,1} = I_r \frac{R-r}{r} + R \cdot \cos(\alpha - \beta) \cdot [(R-r)m_r + h \cdot m_a] - (I_a + m_a \cdot h^2 + m_r \cdot (R-r)^2)$$

$$M_{2,2} = I_a + m_a \cdot h^2 + m_r \cdot (R-r)^2 \cdot I_r \cdot \left(\frac{R-r}{r}\right)^2$$

$$C_{1,1} = R \cdot \sin(\alpha - \beta) \cdot (\dot{\alpha} - \dot{\beta}) \cdot [(R-r) \cdot m_r + h \cdot m_a]$$

$$C_{1,2} = -R \cdot \sin(\alpha - \beta) \cdot (\dot{\alpha} - \dot{\beta}) \cdot [(R-r) \cdot m_r + h \cdot m_a]$$

$$C_{2,1} = 0; \quad C_{2,2} = 0$$

$$h_1 = -g \cdot \sin(\alpha - \beta) \cdot (R-r) \cdot m_r + h \cdot m_a$$

$$h_2 = g \cdot \sin(\alpha - \beta) \cdot (R-r) \cdot m_r + h \cdot m_a$$

$$t_1 = -F \cdot R - C_t; \quad t_2 = \frac{R}{r} \cdot C_m - C_o$$

$$C_o = A \cdot \mathrm{Sign}(\dot{\alpha}) + B \cdot \dot{\alpha}; \quad C_m = \frac{K_e}{R_e}(V_n - K_e \cdot \omega_r)$$

The torque delivered by the drive motor C_m can be evaluated using the characteristic of the dc brush motor and C_t is defined through Eqs. (1) and (2).

Equation (8) provides a second-order description of the robot dynamics and it can be manipulated for control and planning purposes using the classical methods known in literature for nonlinear systems [2,3]. Here, the knowledge of the dynamics of the vehicle is exploited to develop a tactile sensor for terrain parameter estimation.

2.1.1 Numerical Integration. In order to evaluate the feasibility of employing the CMR as a tactile sensor, a set of simulations was performed. It was assumed an open-loop velocity control with the vehicle starting from a standing condition with the WD in vertical posture; the following parameter set was used: R =80 mm, r=18 mm, V_n=5 V, h=62 mm, m_c=0.3 kg, m_r =1.1 kg. The value for the rolling resistance coefficient f_t for different terrains was experimentally determined as described later in Sec. 4. The numerical integration was performed using the fourth order Runghe–Kutta algorithm with a maximum time step of 1 ms.

A representative result is shown in Fig. 3, where the plots of the vehicle linear velocity and the WD swing angle within the cylindrical shell are shown for a run on sandy soil.

Note that the vehicle shows a starting transient state during which the WD behaves like a pendulum, followed by a steady-state condition during which the robot rolls with constant velocity and the WD holds a constant swing angle balancing the rolling resistance due to terrain interaction. The vehicle adapts its kinematics according to the terrain that it is traversing. For example, given a desired velocity, the vehicle will travel with larger swing angle and drive torque on a sandy soil rather than on a rigid surface. This suggests the potential application of the vehicle for sensing terrain characteristics.

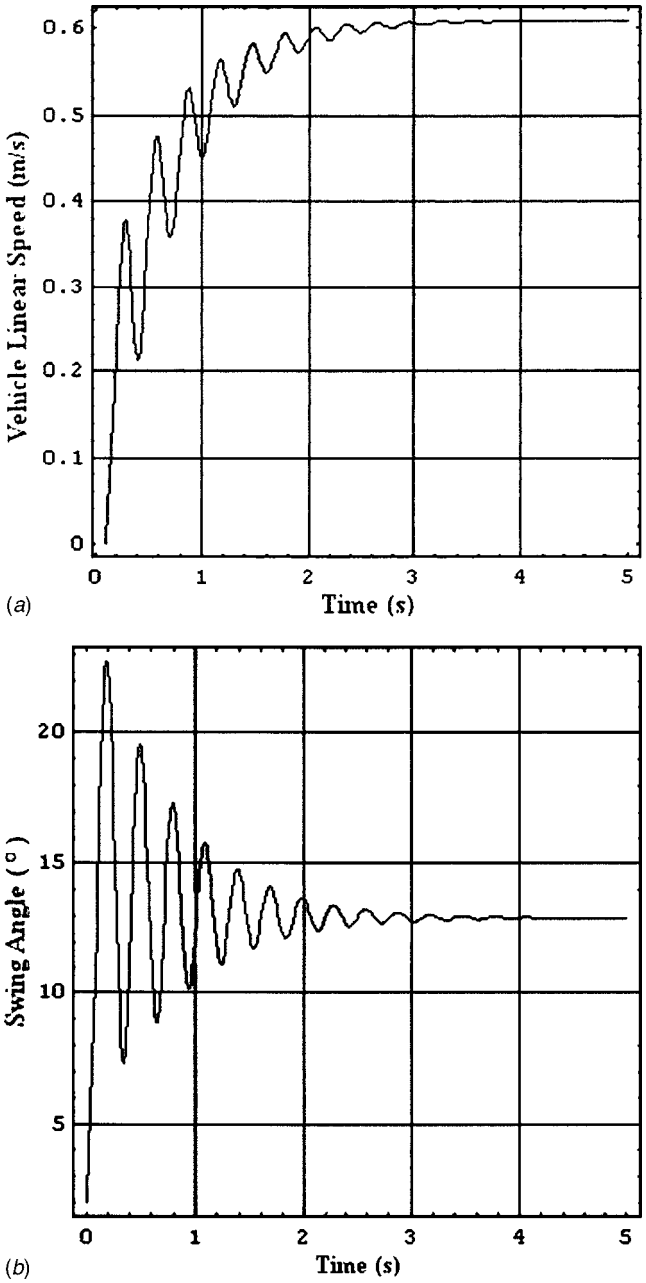

Fig. 3 Results from a typical simulation: (*a*) linear speed of the CMR, (*b*) swing angle of the internal WD

2.2 Mechanics of Vehicle-Terrain Interaction. In this section, the mechanics of vehicle-terrain interaction is studied following a local approach according to the classical theory of Terramechanics. The purpose of this study is to analyze the influence of the local properties of the terrain on the behavior of the vehicle and to develop a method for estimating key terrain parameters by observing the vehicle's motion. External shell-terrain interaction has been shown to play a significant role in rough-terrain mobility [6,7]. The case of a rigid wheel on deformable terrain is examined, as this is the expected condition for our vehicle. Note, however, that this problem is of more general interest as it might be extended to the pneumatic tires-terrain mechanics, since a pneumatic tire will behave like a rigid rim on soft terrain [6].

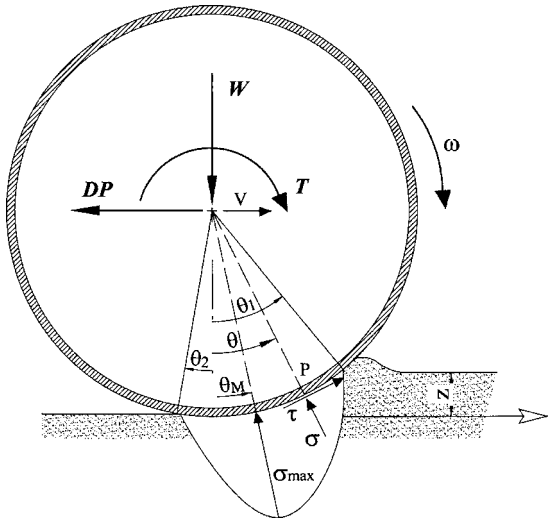

Fig. 4 Stress region at the vehicle-terrain interface, adapted from [6]

A free-body diagram of a dynamically equivalent system traveling on deformable terrain is shown in Fig. 4. A steady-state motion with the vehicle rolling at constant speed is assumed. A drive torque T is applied to the vehicle axis by the unbalancing of the weight force of the WD and balances the external load caused by the motion resistance offered by terrain. Note that only a vertical load W is applied to the vehicle and no horizontal force (drawbar pull) is present during the steady-state motion thanks to the special architecture of the vehicle which can work as a "single wheel" system. The external shell has angular velocity ω, and its center possesses a linear velocity v. The angle from the vertical at which the wheel first makes contact with the terrain is denoted with θ_1. The angle from the vertical at which the wheel loses contact with the terrain is denoted with θ_2. Thus, the entire angular wheel-terrain contact region is defined by $\theta_1+\theta_2$. A stress region is created at the wheel-terrain interface; at a given point on the interface, the stress can be decomposed into a component acting normal to the wheel, σ, and a component acting parallel to the wheel, τ. A semiempirical expression for the normal stress as a function of the angle θ has been proposed by Bekker [6] as

$$\sigma(z) = (k_c + k_\varphi \cdot b) \cdot \left(\frac{z}{b}\right)^n \tag{9}$$

Janosi and Hanamoto [10] formulated an expression for estimating empirically the shear stress, given by

$$\tau(\theta) = (c + \sigma(\theta) \cdot \tan\varphi) \cdot (1 - e^{-R/k\cdot(1-i)\cdot(\sin\theta_1 - \sin\theta)}) \tag{10}$$

where k is the shear deformation modulus, R is the shell radius, i is the vehicle slip defined as $i=1-(V/R\omega)$, z is the vertical sinkage, b the vehicle's width, and k_c, k_φ and n are the sinkage coefficients.

The parameters c and φ characterize the behavior of a given terrain and are defined, respectively, as cohesion and internal friction angle. Cohesion of the material is the bond that cements particles together irrespective of the normal pressure exerted by one particle upon the other. On the other hand, particles of frictional masses can be held together only when a normal pressure exists between them. The knowledge of c and φ would allow to estimate the maximum terrain shear strength that a given wheel-terrain system can generate and to assess terrain traversability according to the Coulomb–Mohr soil failure criterion. This criterion postulates that the material at a given point will fail if the shear stress satisfies the following condition

$$\tau \geq \tau_{\text{Max}} = (c + \sigma_{\max} \cdot \tan\varphi) \tag{11}$$

3 The CMR as a Tactile Sensor

In this section, we discuss a potential application of the CMR as a tactile sensor for estimating terrain metric. Global and local properties of a given terrain can be estimated observing the vehicle's motion through multi-sensor measurements. The global motion resistance C_t offered by a terrain can be measured during the steady-state motion of the vehicle using Eq. (8) which takes the shape of

$$C_t(\omega) = \frac{R}{r} \cdot C_m(\omega) - C_o(\omega) \tag{12}$$

C_o is the resistance due to internal frictions and C_m is the drive torque that can be estimated with reasonable accuracy from the electrical current drawn by the drive motor, since torque is roughly proportional to current. The organic rolling resistance C_o can be estimated running some experiments on flat and rigid surface where C_t is negligible. The rolling angular speed ω of the vehicle can be computed by a vision-based measurement using an external camera [11] (see Sec. 4). In order to estimate local key terrain parameters, the dynamic equilibrium of the vehicle can be expressed in terms of the local stresses σ and τ [see Eqs. (9) and (10)]. The physical parameters of interest are the terrain cohesion c and the internal friction angle φ. As shown in Fig. 4, the vertical load W and the equivalent drive torque T applied to the vehicle are balanced by the stress region beneath the wheel according to the following equilibrium equations:

$$W = R \cdot b \cdot \left(\int_{\theta_1}^{\theta_2} \sigma(\theta) \cdot \cos\theta \cdot d\theta + \int_{\theta_1}^{\theta_2} \tau(\theta) \cdot \sin\theta \cdot d\theta \right) \tag{13}$$

$$DP = R \cdot b \cdot \left(\int_{\theta_1}^{\theta_2} \tau(\theta) \cdot \cos\theta \cdot d\theta - \int_{\theta_1}^{\theta_2} \sigma(\theta) \cdot \sin\theta \cdot d\theta \right) \tag{14}$$

$$T = R^2 \cdot b \cdot \int_{\theta_1}^{\theta_2} \tau(\theta) d\theta \tag{15}$$

In the following analysis the vertical load W and the torque T are assumed to be known quantities. The vertical load W can be computed from a static analysis of the vehicle mass, which is valid due to the steady-state motion and the torque T equals the rolling resistance C_t. The vehicle slip i in Eq. (10) can be estimated from an external camera. The numerical integration of Eqs. (13)–(15) yields the three unknown quantities c, φ and θ_1; the effect of rut recovery is neglected ($\theta_2=0$). Note that two assumptions are made to solve Eqs. (13)–(15). The first is that the maximum shear and normal stress occur at the same location θ_M (see Fig. 4). The second assumption is that the angular location of maximum stress θ_M occurs midway between θ_1 and θ_2, i.e., $\theta_M=(\theta_1+\theta_2)/2$. Analysis and simulation have shown that both assumptions are reasonable for a wide range of soils with low to moderate slip ratios [7].

4 Experimental Results

In this section, the dynamic model of the vehicle is experimentally validated using the cylindrical shaped prototype shown in Fig. 5(*a*). The CMR is also proved to be effective in experimental trials serving as a tactile sensor for terrain estimation. All the experiments were performed employing the multi-terrain testbed shown in Fig. 5(*b*).

4.1 Experimental Model Validation. The motion of the vehicle as predicted by the dynamic model was experimentally validated. Figure 6 shows the velocity of the CMR as obtained from analytical and experimental data for a typical run on sand. The

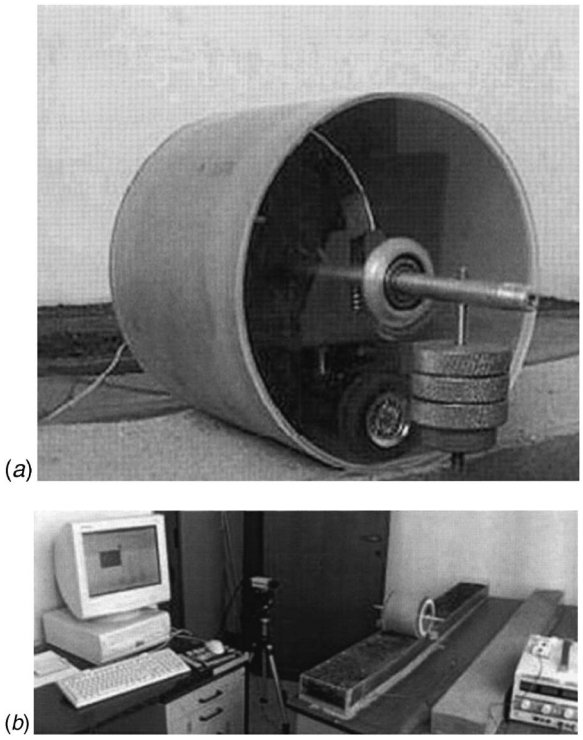

Fig. 5 The cylindrical prototype (*a*), and the multi-terrain testbed (*b*)

data match very well; small discrepancies remain due to the irregularities of sand in experiments and noise in the visual measurements. The steady-state vehicle speed as foreseen by the model was also compared with that derived by the vision-based motion estimation module for different voltage supplies. The results are collected in Fig. 7. Each experimental data is the average value obtained by five similar tests. A good agreement of the dynamic model with experimental data can be observed; the discrepancy is always within 3%.

4.2 Terrain Characterization. Experiments were performed to estimate the rolling resistance C_t offered by various terrains. Dry sand, agricultural terrain, red terrain, and dry peat were tested under different vehicle velocities and weights. Soil surface was relatively leveled and compacted before each run. The estimated values of f_t are collected as function of the vehicle's angular velocity in Fig. 8 along with the fitted quadratic regressions. Table 1 collects the values of f_o and f_s for each tested terrain.

Key soil parameters for sand were also measured. The sinkage coefficients in Eqs. (9) and (10) for compact sand were adopted from [12]: $n=1.1$, $K_c=24$ kN/m^2, $K_\varphi=1528$ kN/m^3. The average values measured for cohesion and friction are collected in Table 2 and they match the available published data very well [13]. The experimental framework for terrain estimation produces good results and the vehicle could serve as a tactile sensor.

5 Conclusions

A cylindrical shaped mobile robot was introduced and its mobility on deformable, soft terrain was studied from a theoretical and experimental prospect. A comprehensive dynamic model of the rolling motion of the vehicle was described taking into account the vehicle-terrain interaction. The model was shown to be effective in experimental trials performed on a prototype operating on a multi-terrain testbed. An unconventional application of the cylindrical mobile robot as a tactile sensor for terrain param-

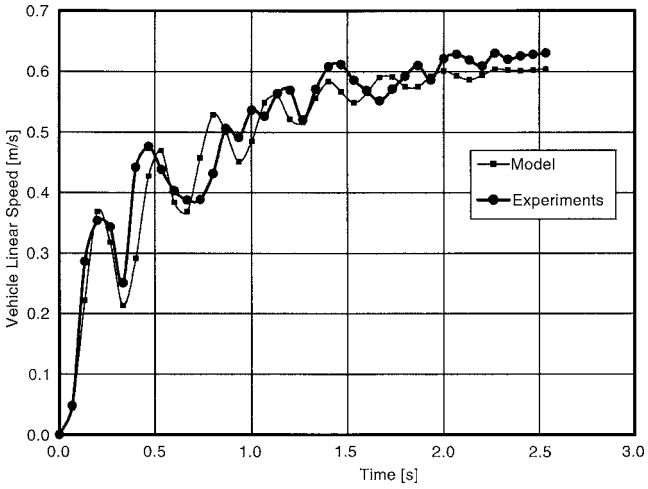

Fig. 6 Plot of the vehicle's speed as derived by the experimental and analytical data

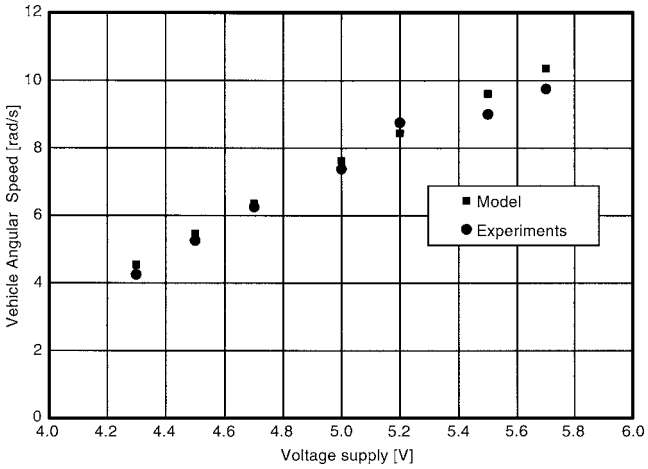

Fig. 7 Comparison of the model with experimental data for steady-state motion

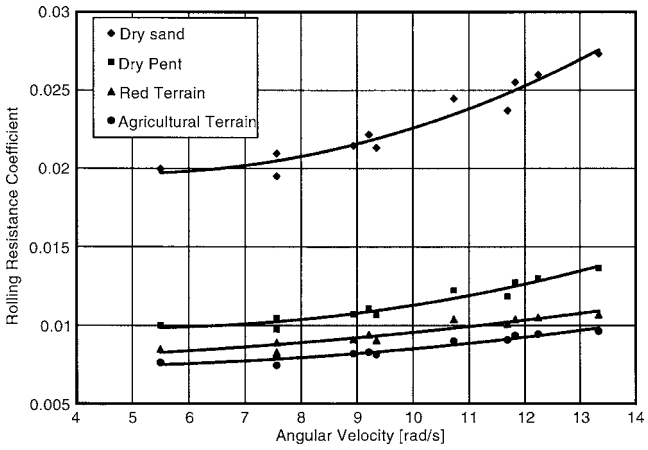

Fig. 8 Correlation of f_t with the vehicle's rolling velocity for different terrains

Table 1 Basic and speed effect coefficient for different terrains

Terrain	f_o	f_s (s^2/rad^2)
Sand	0.092	$0.28 \cdot 10^{-3}$
Dry peat	0.045	$0.12 \cdot 10^{-3}$
Red terrain	0.037	$0.15 \cdot 10^{-3}$
Agricultural terrain	0.028	$0.098 \cdot 10^{-3}$

Table 2 Key terrain parameters for sand

	Terrain parameters for sandy soil	
Parameter	Measured data	Published data
Cohesion [kPa]	0.7	0–1.0
Internal friction [°]	30	25–32

eter estimation was investigated based on observing the vehicle's behavior through multi-sensor measurements. The methods described in this paper can be used to enhance mobility through integration with conventional control and planning algorithms.

References

[1] Halme, J., Schönberg, T., and Wang, Y., 1996, "Motion Control of a Spherical Mobile Robot," *Proc. IEEE Workshop on Advanced Motion Control*, Mie, Japan, pp. 259–264.

[2] Bicchi, A., Balluchi, A., Prattichizzo, D., and Gorelli, A., 1997, "Introducing the Sphericle: An Experimental Testbed for Research and Teaching in Nonholonomy," *Proc. IEEE Intern. Conf. on Robotics and Automation*, Albuquerque, New Mexico, pp. 2620–2625.

[3] Bhattacharya, S., and Agrawal, S., 2000, "Design, Experiments and Motion Planning of a Spherical Rolling Robot," *Proc. Intern. Conf. on Robotics and Automation*, San Francisco, CA, pp. 1207–1212.

[4] Drenner, A., Burt, I., Dahlin, T., Kratochvil, B., McMillen, C., Nelson, B., Papanikolopoulos, N., Rybski, P. E., Stubbs, K., Waletzko, D., and Yesin, K. B., 2002, "Mobility Enhancements to the Scout Robot Platform," *Proc. of the 2002 IEEE Intern. Conf. on Robotics and Automation*, Washington, D.C., May 11-15, pp. 1069–1074.

[5] Xu, Y., Brown, H. B., and Au, K. W., 1999, "Dynamic Mobility With Single-Wheel Configuration," Int. J. Robot. Res., **18**(7), pp. 728–738.

[6] Bekker, G., 1969, *Introduction to Terrain-Vehicle Systems*, University of Michigan Press, Ann Arbor, MI.

[7] Iagnemma, K., and Dubowsky, S., 2004, *Mobile Robots in Rough Terrain*, Springer Tracts in Advanced Robotics, Springer, Berlin, Germany.

[8] Brooks, C., Iagnemma, K., and Dubowsky, S., 2005, "Vibration-based Terrain Analysis for Mobile Robots," *Proc. of the 2005 IEEE International Conf. on Robotics and Automation*, Barcelona, Spain, April 18-22, pp. 3415–3420.

[9] Reina, G., 2004, "Rough Terrain Mobile Robot Localization and Traversability With Applications to Planetary Explorations," Ph.D. thesis, Politecnico of Bari, Bari, Italy.

[10] Janosi, B., and Hanamoto, B., 1961, "Analytical Determination of Drawbar Pull as a Function of Slip for Tracked Vehicles in Deformable Soils," *Proc. of the First Int. Conf. On Terrain-Vehicle Systems*, Minerva Tecnica, ed. Turin, Italy.

[11] Reina, G., Foglia, M. M., Milella, A., and Gentile, A., 2004, "Dynamic Modeling for a Cylindrical Mobile Robot on Rough-Terrain," *Proc. of the 2004 ASME IMECE*, November 14–19, Anaheim, CA.

[12] Onafeko, O., and Reece, A., 1967, "Soil Stresses and Deformation Beneath Rigid Wheels," J. Terramech., **4**(1), pp. 59–80.

[13] Wong, J., 1993, *Theory of Ground Vehicles*, Wiley, New York.